Computers in Biology and Medicine 121 (2020) 103827

Contents lists available at ScienceDirect

Computers in Biology and Medicine

journal homepage: http://www.elsevier.com/locate/compbiomed

An agent-based model to evaluate the COVID-19 transmission risks in facilities

Erik Cuevas

Departamento de Electrónica, Universidad de Guadalajara, CUCEI, Av. Revolución 1500, Guadalajara, Jal, Mexico

ARTICLE INFO

Keywords:
COVID-19
Agent-based modeling
Transmission models

ABSTRACT

The rapid spread of the coronavirus disease (COVID-19) has become a global threat affecting almost all countries in the world. As countries reach the infection peak, it is planned to return to a new normal under different coexistence conditions in order to reduce the economic effects produced by the total or partial closure of companies, universities, shops, etc. Under such circumstances, the use of mathematical models to evaluate the transmission risk of COVID-19 in various facilities represents an important tool in assisting authorities to make informed decisions. On the other hand, agent-based modeling is a relatively new approach to model complex systems composed of agents whose behavior is described using simple rules. Different from classical mathematical models (which consider a homogenous population), agent-based approaches model individuals with distinct characteristics and provide more realistic results. In this paper, an agent-based model to evaluate the COVID-19 transmission risks in facilities is presented. The proposed scheme has been designed to simulate the spatiotemporal transmission process. In the model, simulated agents make decisions depending on the programmed rules. Such rules correspond to spatial patterns and infection conditions under which agents interact to characterize the transmission process. The model also includes an individual profile for each agent, which defines its main social characteristics and health conditions used during its interactions. In general, this profile partially determines the behavior of the agent during its interactions with other individuals. Several hypothetical scenarios have been considered to show the performance of the proposed model. Experimental results have demonstrated that the simulations provide useful information to produce strategies for reducing the transmission risks of COVID-19 within the facilities.

1. Introduction

On January 30, 2020, the World Health Organization declared the coronavirus disease 2019 (COVID-19) outbreak as a Public Health Emergency of International Concern. As of April 10, 2020, there are 1,684,833 laboratory-confirmed cases of the virus and 102,136 deaths reported globally.

COVID-19 is considered a very infectious disease [1] transmitted from one host to another through different modes of transmission, such as airborne droplets disseminated by sneezing or coughing, direct physical contact, etc. In its transmission, an agent or set of agents are introduced into a population of susceptible elements. Then, the infection is transferred to other agents through its forms of transportation, consequently spreading in the population. An infected element can persist without typical symptoms at the early phase of the infection [2]; only later, the patient can develop clinical symptoms and be diagnosed as a disease case. When the amount of cases increases above the normal average of events within a brief period, a disease outbreak happens.

Several mathematical tools are used to characterize, predict, or analyze the transmission process of an infectious disease [3]. Traditional explorative methods use experimental and statistical data for obtaining information on the disease transmission process. However, such approaches are not appropriate [4] for several reasons: a) For human infectious diseases, large-scale tests may be impractical or unethical and b) available data sets pertinent to the disease include only partial information not accurate enough for reliable statistical studies.

Mathematical modeling is recognized as an important tool for emulating the transmission of infectious diseases computationally. Mathematical models have been widely used for evaluating the effectiveness of control strategies and for reducing their associated risks [5]. Through mathematical modeling, it is possible to obtain critical information about the mechanisms of transmission and spread. It helps to highlight important factors in the disease transmission process. From its results, it is also possible to suggest preventive measures or effective

---

E-mail address: erik.cuevas@cucei.udg.mx.

https://doi.org/10.1016/j.compbiomed.2020.103827
Received 18 April 2020; Received in revised form 15 May 2020; Accepted 16 May 2020

control strategies. Another important function of mathematical models is hypothesis testing [6]. Under this role, it is possible to test different scenarios considering distinct hypothetical conditions that are impossible to analyze in the real circumstances. Compared to experimental methods, the modeling schemes have the convenience of saving time and economic resources. In the last decades, the design of mathematical models for disease transmission has attracted the attention of the scientific community. Some examples include the classical Susceptible-Infect- Susceptible (SIS) epidemic model established by Kermack and McKendrick [7], the Susceptible-Infect-Recovered (SIR) epidemic model proposed by Bailey [8], the Susceptible-Infect-Vaccination-Susceptible (SIVS) epidemic system introduced by Arion et al. [9] and the stochastic Susceptible-Infect-Quarantine-Susceptible (SIQS) epidemic model studied by Zhang et al. [10]. All these models are proper for explaining the global behavior of an epidemic on larger scales considering general variables. They are not able to provide accurate predictions at a finer resolution. There exist many scenarios in which it is important to analyze the transmission dynamics in a more microscopic way, especially in small populations or in facilities where the infection process can be identified by the interactions among their members [11].

In order to obtain better conclusions from processes, simple models are no longer enough to analyze them. The wide availability of fast computing resources has allowed the construction and analysis of more complex models. Under such conditions, it has emerged a new field of knowledge known as complex systems [12]. In complex systems, it is studied how systems affect individual behaviors, especially when such individuals have the capacity to influence these systems. In these systems, complex behaviors of higher-level organizations appear as a consequence of the collective interaction of individuals that participate in a self-organizing process [13].

Agent-based modeling [14] represents a new paradigm to model complex systems using agents or elements. Agents maintain behaviors that are described by simple rules and influenced by the collective interaction with other agents. Under this paradigm, global behavioral patterns that have not been directly programmed emerge through the collective interaction among agents. Agent-based models attempt to relate how global regularities may emerge through processes of collective cooperation. Under this scheme, a population of agents maintains a behavior characterized by a set of simple rules. The objective of such rules is to emulate the individual movements of real actors when they interact with their local environment. Although the system is modeled from the individual point of view, its main properties are visualized from a global perspective. The powerful modeling characteristics of the Agent-based models have motivated their use in several applications which include the behavior in supply chains [15] and the stock market [16], the characterization of the immune system [17], the understanding about the fall of ancient civilizations [18], the consumer purchasing behavior [19], to name a few. Agent-based models have also been used as an alternative to classical mathematical tools to describe the behavior of diseases. These approaches produce better results in conditions where it is required to determine the dynamics of a disease in a more fine-context way, particularly when it is necessary to characterize the transmission process person-to-person [20]. As a result, several agent-based schemes have been proposed to model how the uncertainties in disease transmission change according to different characteristics of the population and affects the overall behavior of epidemics [20,21]. Some examples include studies such as [22] where it is used historical information to produce contact patterns in agent-based approaches with the objective to characterize the behavior of previous critical epidemics. In contrast, in Ref. [23], historical data are considered to evaluate the possibilities of future disease outbreaks. In Ref. [24], it is integrated empirical mobility data models to emulate the diffusion dynamics of global disease without considering the transmission at the level of individuals. More recently, in Ref. [25,26], it is proposed two agent-based schemes which model individual contact to capture the nationwide spread of influenza in Australia and Switzerland, respectively. Both models generate an artificial population considering census data. Then, agents are influenced by some operators that simulate the transmission of influenza through the interaction of agent groups.

Several important measurements have been emitted as a general way of limiting COVID-19 infection. Inside facilities, it is presented a high probability of infection. Within these spaces, it is maintained a high contact rate between people sharing the same common surfaces of interaction. However, rarely there are no specific countermeasures related to these facilities nor conducted studies that analyze possible coexistent strategies. The public health consequences of acquiring COVID-19 have led many governments to impose a set of control measures. As the countries reach the infection peak, it is planned to return to the normality under new coexistence conditions in order to reduce the economic effects produced by the total or partial closure of companies, universities, shops, etc. Under such circumstances, the use of mathematical models to evaluate the transmission risk of COVID-19 in this type of facility represents an important tool in assisting authorities to make informed decisions. In this paper, an agent-based model to evaluate the COVID-19 transmission risks in facilities is presented. In the model, the behavior of each individual is characterized by a set of simple rules that considers its basic interactions inside the facility. In its iterations, each agent maintains different mobility requirements and contagion susceptibility. From these models, several possible scenarios can be tested to obtain the coexistence conditions that need to be imposed among the members or the habits that have to be avoided for reducing the transmission risks. Different from classical mathematical models, agent-based approaches model individuals with distinct characteristics such as mobility needs, grouping requirements, or a variety of health conditions providing more realistic results.

This paper is organized as follows: In Section 2, the basic concepts of agent-based modeling are introduced. In Section 3, the proposed model is explained. In Section 4, the experimental results are exposed. In Section 5, the results and characteristics of the proposed method are discussed. Finally, in Section 6, conclusions are drawn.

2. Agent-based modeling

Agent-based modeling corresponds to a new scheme for simulating systems with interacting autonomous elements. Agents are artificial individuals programmed to perform pre-defined operations [27]. While they operate based on their own behavior, collaborate, or compete with each other agents. The complexity of the actions conducted by an agent is quite simple. They range from elementary decisions (yes or no) to stochastic behaviors.

Agents interact in an environment (virtual map) in the form of a lattice or a multi-dimensional space. Agents can move freely within the environment. With this characteristic, it is possible to visualize the agent behaviors as a physical system, such as simulations of evacuations, traffic, biological systems, infections, etc.

Agent-based models are simple. They do not use sophisticated architectures or difficult behavioral rules. In spite of these simple behaviors, they are capable of generating several complex global patterns (behaviors) as a consequence of the modeling characteristics produced by the interactions of a set of simple agents. Global behavioral patterns refer to consistent microscopic regularities, such as coherent temporal, spatial and behavioral structures, or identifiable distributions.

A general agent-based modeling scheme consists of the following steps. First, a set of A agents $\{\mathbf{a}_1, \ldots, \mathbf{a}_A\}$ are initialized. Under this stage, agents are configurated in a determined position or in a specific state. Then, each agent $\mathbf{a}_i$ $(i \in 1, \ldots, A)$ is selected randomly or considering a particular order. For this agent $\mathbf{a}_i$, a set of rules are applied in order to change its position, state or relationship with other agents. These rules consider a relation of conditions imposed by other agents (specific agents) or local influences (neighbor agents). This process is repeated until a determined stop criterion has been reached.

Under the agent-based methodology, several interesting basic global patterns have been proposed to simulate complex phenomena such as diffusion, concentration and insolating, fire spreading, segregation and others. These behavioral patterns have been analyzed in terms of the simple rules that provoke them. In order to illustrate this methodology, two simple examples are considered: Fire spreading and segregation.

2.1. *Fire spreading*

In fire spreading [12], the objective is to emulate the way in which fire moves through a zone of trees distributed with different densities. Fire, in the real world, does not spread under deterministic principles. From one tree to another tree, fire is transmitted based on a variety of elements such as the type of wood, wind, and how close the branches are to each other. Agent-based modeling allows emulating systems with many interconnected factors that affect a process. Under agent-based modeling, the fire spreading phenomenon is simulated by considering the following procedure. First, a lattice of $M \times N$ agents $\{\mathbf{a}_1, \ldots, \mathbf{a}_{M\times N}\}$ is randomly initialized. Each agent represents a tree or an empty space. One random agent $\mathbf{a}_R$ of the lattice is considered the location in which starts the fire. Considering this agent $\mathbf{a}_R$, the next rule is applied. In the neighborhood of $\mathbf{a}_R$, a new agent $\mathbf{a}_S$ is randomly selected. Then, with a probability p it is assumed that the fire is transmitted to $\mathbf{a}_S$. Otherwise, the tree remains unburned. This process is repeated until all possible trees become burned. Fig. 1 shows the visual results produced by the fire spreading agent-based model obtained in three different stages.

2.2. *Segregation*

Schelling proposed an agent-based model to emulate the segregation phenomenon [28,29] with the objective of providing an explanation for why people that maintain different ethnic origins tend to segregate geographically. In the model, two different types of agents $\mathbf{A} = \{\mathbf{a}_1, \ldots, \mathbf{a}_{A/2}\}$ and $\mathbf{B} = \{\mathbf{b}_1, \ldots, \mathbf{b}_{A/2}\}$ are randomly distributed in a finite two-dimensional space. In each step, the following rule is considered. A random agent from $\mathbf{A}$ or $\mathbf{B}$ is selected. Then, it is counted the number of agents of the same type around its neighborhood. If the fraction of agents of the same type is below a threshold Th, it moves to another position randomly chosen in the space.

The rule for this model is quite simple. Schelling discovered with this model how high the Th value had to be in order to occur segregation. It seems reasonable to assume that segregation requires high homophilic characteristics (high Th values). However, Schelling demonstrated that segregation phenomenon could happen with much lower Th values. Fig. 2 shows the visual results produced by the segregation agent-based model obtained in three different stages. Fig. 2 was used from [29] with permission. It represents a reconstruction from the original figure, which appeared in [28].

3. The proposed agent-based model

In this section, the proposed agent-based model to evaluate the COVID-19 transmission risks in facilities is explained. The agent-based model has been developed to emulate the transmission process from an agent perspective. The approach allows highlighting the importance of individual contact patterns in the modeling. Therefore, this scheme makes it also possible to analyze strategies at a micro-scale.

The disease of COVID-19 is transmitted through different mechanisms, which include hand contamination followed by mucosal inoculation [30], and droplets or aerosols disseminated by coughing and sneezing [31]. The measures considered to avoid the transmission of COVID-19 involve simple habits such as washing one's hands continuously, sneezing into one's hand or elbow, using a face mask and maintaining low mobility. The section is divided into two parts: (3.1) model description and (4.2) the computational procedure.

3.1. *Model description*

The probability of a person being infected depends on several factors that range from his health condition to his discipline in following the prevention measurements. In our approach, the probability of infection is modeled through the use of a probability term *Pri*. This term is different for each individual and summarizes all possible factors that affect positively or negatively to his infection.

The infection maintains a high relationship with the contact and mobility rate among the people in the facility. In the proposed scheme, the contact and mobility rate among elements is modeled with a probability factor *Prcm*. This parameter involves several factors that determine the movement of an individual within the facility, such as jobs assigned, number of classrooms for a student, etc. This parameter can be the same for groups of individuals, such as workers with the same area, students with the same schedule, etc. However, elements difficult to describe, such as personal intentions, visiting friends of different areas or others, modify this parameter, making it unique for each individual.

3.1.1. *Initialization*

In the proposed model, two different types of agents $\mathbf{A}(k) = \{\mathbf{a}_1(k), \ldots, \mathbf{a}_A(k)\}$ and $\mathbf{B}(k) = \{\mathbf{b}_1(k), \ldots, \mathbf{b}_B(k)\}$ are defined. The characteristic of the agents $\mathbf{A}$ and $\mathbf{B}$ can change in each iteration k of the simulation. The agents from $\mathbf{A}$ represent the population of A susceptible elements in the facility while the agents from $\mathbf{B}$ correspond to the B infected individuals. In each, iteration the number of agents in $\mathbf{B}$ determines the number of infected individuals inside the facility. In the first iteration ($k = 1$), the model starts generating the positions of each agent $\mathbf{a}_i$ and $\mathbf{b}_j$ ($i \in 1, \ldots, A; j = 1, \ldots, B$) which are initialized with random positions in a *two*-dimensional space ($\mathbf{a}_i(k) = \{a_{i,x}(k), a_{i,y}(k)\}$, $\mathbf{b}_j = \{b_{j,x}(k), b_{j,y}(k)\}$). In this process, each coordinate of $a_{i,d}$ and $b_{j,d}$ ($d \in [x, y]$) is set with a numerical value uniformly determined between the defined lower (L_x, L_y) and upper (U_x, U_y) limits, so that

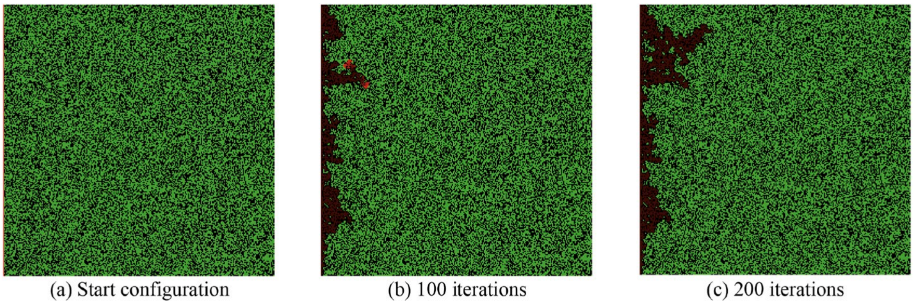
(a) Start configuration (b) 100 iterations (c) 200 iterations

Fig. 1. Visual results produced by fire spreading agent-based model obtained in three different stages.

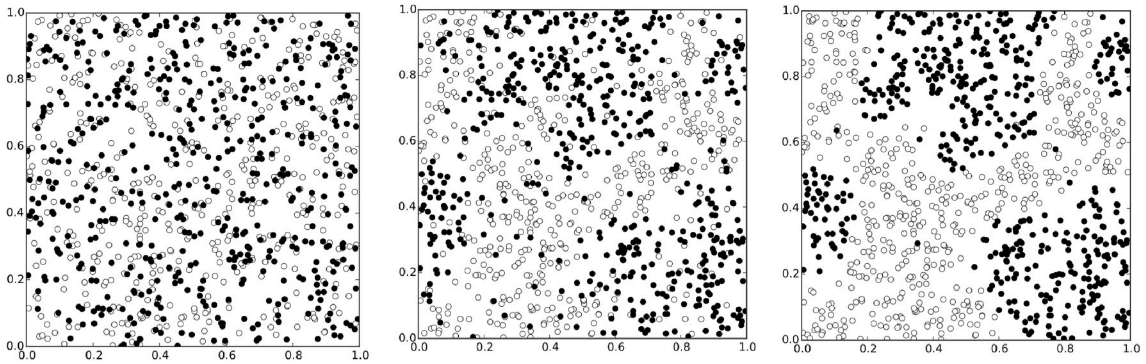

(a) Start configuration (b) 100 iterations (c) 200 iterations

Fig. 2. Visual results produced by the segregation agent-based model obtained in three different stages. This graph is republished from the work of Professor Hiroki Sayama [29], with permission. The figure has been slightly modified in that the iterations have been added to show the evolution of the simulation process. These iterations have been incorporated only for illustration proposes.

$$\begin{aligned} a_{i,d},(1) &= L_d + \mathrm{rand}(0,1)\cdot(U_d - L_d) \\ b_{j,d}(1) &= L_d + \mathrm{rand}(0,1)\cdot(U_d - L_d) \end{aligned} \tag{1}$$

where $\mathrm{rand}(0,1)$ is a function that delivers a random number within a uniform distribution $U[0,1]$ between 0 and 1. U_d and $L_d$symbolize the lower and upper bounds, respectively (where $d \in [x,y]$).

To each agent $\mathbf{a}_i (i \in [1, A])$ from **A**, it is assigned a probability of infection Pri_i which ranges from zero to one. With the value of Pri_i, it is possible to emulate different scenarios for the agent $\mathbf{a}_i$ such as its immunity (values near to zero), a normal transmission rate (around 0.2) or a high susceptibility (values near to one). In order to provide a realistic effect in the simulation, it is important that the population **A** presents heterogeneity. For this propose, the values of $Pri_i$are randomly set with numbers uniformly distributed within the pre-specified lower (l_{in}) and upper (u_{in}) limits. Values close to the limit l_{in} represents agents with good immunity health conditions or people that are accustomed to being disciplined with the prevention measurements. Values close to the limit u_{in} corresponds to agents with a high susceptibility to be infected.

To each agent $\mathbf{a}_i$ and $\mathbf{b}_j$ ($j \in [1, B]$) from **A** and **B**, respectively, it is assigned a contact or mobility probability $Prcm_i^{\mathbf{A}}$ and $Prcm_j^{\mathbf{B}}$which ranges from zero to one. With the values of $Prcm_i^{\mathbf{A}}$ and $Prcm_j^{\mathbf{B}}$, it is possible to simulate distinct classes of contact or mobility for susceptible (**A**) and infected (**B**) elements. Values of $Prcm_i^{\mathbf{A}}$ and $Prcm_j^{\mathbf{B}}$ near to zero corresponds to susceptible and infected agents with poor contact and mobility within the facility. On the contrary, values near one imply agents with high mobility. For realistic results, the values of $Prcm_i^{\mathbf{A}}$ and $Prcm_j^{\mathbf{B}}$can be randomly set with numbers uniformly distributed within the pre-specified lower (l_{cm}) and upper (u_{cm}) limits according to the mobility characteristics of the facility to be emulated. Values close to the limit l_{cm} represents agents with poor contact and mobility. On the contrary, values close to the limit u_{cm} corresponds to agents with high mobility.

3.1.2. Behavioral rules

In order to simulate the COVID-19 transmission, agents of **A** and **B** maintain behaviors that are characterized by simple rules and influenced by the collective interaction among them. In their behavior, elements from **A** consider a contagious rule or Rule I to define if a certain agent $\mathbf{a}_i$ is infected or not. On the other hand, agents from **A** and **B** are subject to a rule of contact and mobility identified as Rule II.

3.1.2.1. Rule I. In the contagious rule or Rule I, for each agent $\mathbf{a}_i$ from **A** it is analyzed the existence of an infected agent $\mathbf{b}_j$ ($\mathbf{b}_j \in \mathbf{B}$) inside a determined neighborhood R. If this existence is verified, a probabilistic decision process is considered to know if the agent $\mathbf{a}_i$ has been infected or not. Under this process, a random number r is generated within a uniform distribution $U[0,1]$. If the value of r is less than or equal to Pri_i, the agent $\mathbf{a}_i$is considered infected, otherwise, $\mathbf{a}_i$is not contaminated in spite of its contact. The value of R can be used to emulate the permissible contact level under contagious risk. In our scheme, $R = 1$mt; however, this value can be enlarged to allow the possibility of infection with surfaces close to the infected agent. When an agent $\mathbf{a}_i$ is recognized as infected, $\mathbf{a}_i$ is deleted from **A** and added as a new agent $\mathbf{b}_{new}$ within the infected agents in **B**. On the other hand, if none infected agent is detected in the neighborhood R around $\mathbf{a}_i$, then, no action is performed.

Fig. 3 illustrates the operation process of Rule I. In the figure; it is considered a set of 10 (A) susceptible agents and 2 (B) infected elements $\mathbf{A} = \{\mathbf{a}_1, \ldots, \mathbf{a}_{10}\}$ and $\mathbf{B} = \{\mathbf{b}_1, \mathbf{b}_2\}$. The agents are located as it is indicated in Fig. 3(a). From this figure, it is clear that the agents $\mathbf{a}_3$ and $\mathbf{a}_5$ maintain a relationship of closeness (less than the distance R) with $\mathbf{b}_1$ and $\mathbf{b}_2$, respectively. Assuming that the probabilities of infection are $Pri_3 = 0.1$ and $Pri_5 = 0.8$ (an exaggerated value for transmission), it might be that the agent $\mathbf{a}_5$ gets infected since its susceptibility (probability) is really high. On the contrary, as Pri_3 is quite low, the agent $\mathbf{a}_3$remains without the contagious. Fig. 3(b) shows the new configuration of both populations **A** and **B**.

3.1.2.2. Rule II. In Rule II, the contact and mobility of each agent from **A** and **B** are determined. Under this rule, firstly, through a probabilistic test, it is decided if the agent $\mathbf{a}_i$ or $\mathbf{b}_j$ is displaced or if it remains in the same position. For this process, a random number r is generated within a uniform distribution $U[0,1]$. If the value of r is less than or equal to $Prcm_i^{\mathbf{A}}$ or $Prcm_j^{\mathbf{B}}$the new position of the agent $\mathbf{a}_i\,(k+1)$or $\mathbf{b}_j(k+1)$ is modified, otherwise, $\mathbf{a}_i$ or $\mathbf{b}_j$keeps its location $(\mathbf{a}_i\,(k + 1) =$

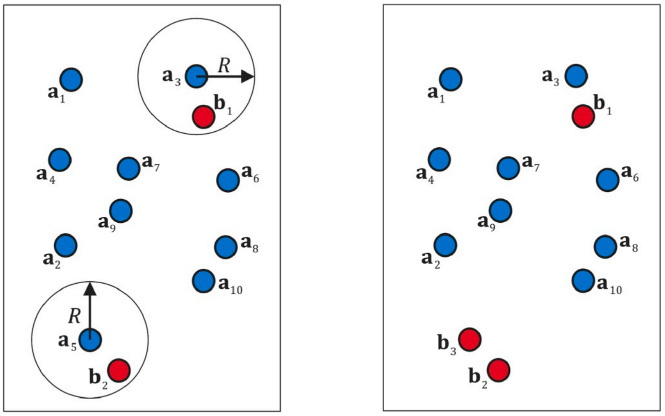

(a) (b)

Fig. 3. Operation of Rule I. (a) initial configuration and (b) final configuration.

$\mathbf{a}_i$ (k) or $\mathbf{b}_j(k+1) = \mathbf{b}_j(k)$).

Once decided on its movement, the model includes two different movement types: local and long-distance displacement. Both movements emulate the basic displacements performed by individuals inside the facilities. Local displacements represent the most frequent movements when individuals interact in their workspace. On the other hand, long-distance displacements refer to movements carried out by the individuals far from their previous position. These movements stimulate actions such as changes in the area, visiting a certain laboratory, cafe break, etc. In order to decide, the movement type performed by the agent $\mathbf{a}_i$or $\mathbf{b}_j$, a probabilistic rule is conducted. The local displacement is executed with a probability of α while a long-distance is applied with a probability of $1-\alpha$. Since local displacements are more frequent than long-distance movements, $\alpha \in [0.6, 08]$.

A local movement is achieved over an agent $\mathbf{a}_i(k)$or $\mathbf{b}_j(k)$ under a probability of α. Local displacements correspond to small displacements achieved around the original positions of an agent $\mathbf{a}_i(k)$or $\mathbf{b}_j(k)$ ($\mathbf{a}_i(k) = \{a_{i,x}(k), a_{i,y}(k)\}$, $\mathbf{b}_j = \{b_{j,x}(k), b_{j,y}(k)\}$). These movements are modeled, adding to the original positions a random number within $[-S, S]$ where S represents the maximal permissible perturbation. The value of S corresponds to the movement performed by the individuals when they interact with their workspace. They are emulated under the following formulation

$$\begin{aligned} a_{i,d}(k+1) &= a_{i,d},(k) + \text{rand}(-1,1)\cdot S \\ b_{j,d}(k+1) &= b_{j,d}(k) + \text{rand}(-1,1)\cdot S \end{aligned} \tag{2}$$

where $d \in [x, y]$ and $\text{rand}(-1,1)$ is a function that delivers a value between -1 and 1, $d \in [x, y]$. In our model, the value of S is set to 2 mts.

A long-distance movement is achieved over an agent $\mathbf{a}_i(k)$or $\mathbf{b}_j(k)$ under a probability of $(1-\alpha)$. Long-distance displacements refer to movements carried out by the individuals far from their previous position. These displacements are emulated through a random change of position for $\mathbf{a}_i(k) = \{a_{i,x}(k), a_{i,y}(k)\}$ or $\mathbf{b}_j = \{b_{j,x}(k), b_{j,y}(k)\}$,so that

$$\begin{aligned} a_{i,d},(k+1) &= L_d + \text{rand}(0,1)\cdot(U_d - L_d) \\ b_{j,d}(k+1) &= L_d + \text{rand}(0,1)\cdot(U_d - L_d) \end{aligned} \tag{3}$$

Fig. 4 illustrates the operation process of Rule II. In the Figure, it is considered a set of 2 (A) susceptible agents and 1 (B) infected element $\mathbf{A} = \{\mathbf{a}_1, \mathbf{a}_2\}$ and $\mathbf{B} = \{\mathbf{b}_1\}$. The agents are located as it is indicated in Fig. 4. It is considered that the agents present the following contact and mobility probabilities $Prcm_1^{\mathbf{A}} = 0.9$, $Prcm_2^{\mathbf{A}} = 0.1$ and $Prcm_1^{\mathbf{B}} = 0.9$. Due to its low probability ($Prcm_2^{\mathbf{A}} = 0.1$), the agent $\mathbf{a}_2$ is not affected by Rule II. For this reason, $\mathbf{a}_2$ $(k+1) = \mathbf{a}_2$ (k). Since the contact and mobility probabilities of $\mathbf{a}_1$ and $\mathbf{b}_1$ are high, they will be operated by Rule II. It is assumed that according to the decision probability of α the agent $\mathbf{a}_1$ is applied a local displacement and the agent $\mathbf{b}_1$ a long-distance movement. Under such conditions, the new position $\mathbf{a}_1$ $(k+1)$ is located around its original position $\mathbf{a}_1$ (k) within a neighborhood S. On the other hand, the new position $\mathbf{b}_1(k+1)$ is determined by a random position inside the facility.

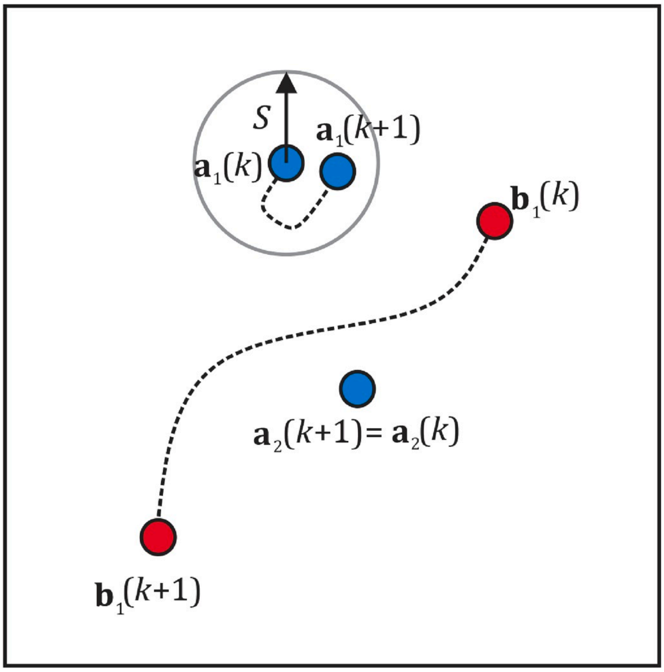

Fig. 4. Operation of rule II.

3.2. Computational procedure

The model to evaluate the COVID-19 transmission risks in facilities has been implemented as an iterative scheme that considers some processes in its operation. In the form of pseudo-code, Algorithm 1 summarizes the operations of the whole process. The model is quite simple and can be coded by using a few lines.

The approach requires as input data the number of susceptible agents A, infected agents B, the pre-specified lower (l_{in}) and upper (u_{in}) infection probability limits, the pre-specified lower (l_{cm}) and upper (u_{cm}) contact and mobility probability limits, the size of the facility $[L_x, U_x\ L_y, U_y]$, the probability of local or long-distance movement α, the maximal permissible perturbation S, and the maximum number of iterations *maxiter*.

The model starts with an initialization stage (Lines 2–4). During this phase, it is configurated the probabilities of infection (Pri_i) for each agent $\mathbf{a}_i(k)$ from $\mathbf{A}$ (line 2) and the contact or mobility probabilities ($Prcm_i^{\mathbf{A}}, Prcm_j^{\mathbf{B}}$) for agents from $\mathbf{A}$ and $\mathbf{B}$ (line 3). The probabilities of infection are randomly obtained from the value l_{in} to u_{in} while the contact or mobility probabilities are random numbers uniformly distributed from l_{cm} to u_{cm}. Then, all agents from $\mathbf{A}$ and $\mathbf{B}$ are located in random positions (line 4) inside the facility.

Algorithm 1. Summarized processes of the proposed model.

After initialization, the model executes the Rule I or infection rule. In rule I (lines 6–14), for each agent $\mathbf{a}_i(k)$ of $\mathbf{A}$, it is analyzed the existence of an infected agent $\mathbf{b}_j$ ($\mathbf{b}_j \in \mathbf{B}$) inside a neighborhood R (line 7). If this existence is verified (F=1, line 8), a probabilistic decision process is considered to know if the agent $\mathbf{a}_i$ has been infected or not (line 9). Under this process, a random number *rand* is generated within a uniform distribution $U[0,1]$. If the value of *rand* is less than or equal to Pri_i, the agent $\mathbf{a}_i$is considered infected, otherwise, $\mathbf{a}_i$is not contaminated in spite of its contact. When an agent $\mathbf{a}_i$ is recognized as infected, $\mathbf{a}_i$ is deleted from $\mathbf{A}$ (line 10) and added as a new agent $\mathbf{b}_{new}$ within the infected agents in $\mathbf{B}$ (line 11). On the other hand, if none infected agent is detected in the neighborhood R around $\mathbf{a}_i$, then, no action is performed.

After Rule I, the rule of contact and mobility or Rule II is executed. Rule I (15–36) is independently applied to agents from $\mathbf{A}$ (lines 15–25) and $\mathbf{B}$ (lines 26–36). For the agents from $\mathbf{A}$, firstly, through a probabilistic test (line 16), it is decided if the agent $\mathbf{a}_i$ is displaced or if it remains in the same position. For this process, a random number *rand* is generated within a uniform distribution $U[0,1]$. If the value of *rand* is less than or equal to $Prcm_i^{\mathbf{A}}$ the new position of the agent $\mathbf{a}_i$ $(k+1)$or $\mathbf{b}_j(k+1)$ is modified, otherwise, $\mathbf{a}_i$ or $\mathbf{b}_j$keeps its location (line 23) ($\mathbf{a}_i$ $(k+1) = \mathbf{a}_i$ (k) or $\mathbf{b}_j(k+1) = \mathbf{b}_j(k)$). Then, another probabilistic test is conducted to know which type of movement will be executed (line 17). Under this test, a random number *rand* is generated within a uniform distribution $U[0,1]$. If the value of *rand* is less than or equal to α a local displacement is applied (line 18); otherwise, a long-distance movement (line 20) is considered. The same set of operations (lines 26–36) is also applied to

Algorithm 1. Pseudo-code for the COVID-19 transmission risk model

```
Input: $A, B, l_{in}, u_{in}, l_{cm}, u_{cm}, [L_x, U_x, L_y, U_y], \alpha, maxiter, R, S, k=1$
                                                                Initialization
$Pri_i \leftarrow$ InitializeProbInf($A, l_{in}, u_{in}$);
$Prcm_i^{\mathbf{A}}, Prcm_j^{\mathbf{B}} \leftarrow$ InitializeProbMob($A, B, l_{cm}, u_{cm}$);
$\mathbf{A}(k), \mathbf{B}(k) \leftarrow$ InitializePos($A, B, [L_x, U_x, L_y, U_y]$);
while $k <= maxiter$ do
                                                                Rule I
For each $\mathbf{a}_i(k) \in \mathbf{A}(k)$
$F \leftarrow$ FindAnInfectedAgentInNeighbor($\mathbf{B}(k), R$);
If $(F == 1)$ then
  If $(rand \le Pri_i)$ then
$\mathbf{A}(k) \leftarrow$ DeleteFromA($\mathbf{a}_i$);
$\mathbf{B}(k) \leftarrow$ IncludeInB($\mathbf{a}_i$);
  end If
end If
end for
                                                                Rule II for A
for each $\mathbf{a}_i(k) \in \mathbf{A}(k)$
If $(rand \le Prcm_i^{\mathbf{A}})$ then
  If $(rand \le \alpha)$
  $\mathbf{a}_i(k+1) \leftarrow$ LocalMovement($\mathbf{a}_i(k), S$);
  else
   $\mathbf{a}_i(k+1) \leftarrow$ LongMovement($[L_x, U_x, L_y, U_y]$);
  end If
else
$\mathbf{a}_i(k+1) = \mathbf{a}_i(k)$
enf If
end for
                                                                Rule II for B
for each $\mathbf{b}_j(k) \in \mathbf{B}(k)$
If $(rand \le Prcm_j^{\mathbf{B}})$ then
If $(rand \le \alpha)$
  $\mathbf{b}_i(k+1) \leftarrow$ LocalMovement($\mathbf{b}_i(k), S$);
else
   $\mathbf{b}_i(k+1) \leftarrow$ LongMovement($[L_x, U_x, L_y, U_y]$);
end If
  else
$\mathbf{b}_i(k+1) = \mathbf{b}_i(k)$
enf If
end for
$k = k + 1$
end while
```

agents from **B**.

The complete process is conducted until the maximal number of generations *maxiter* has been reached. In each, the number of infected agents$|\mathbf{B}(k)|$ in each iteration determines the number of infected individuals inside the facility.

4. Experimental results

In this section, the proposed model is tested under some basic scenarios. The model is flexible and enables testing of several hypotheses. Under this role, it is possible to test different scenarios considering distinct hypothetical conditions that are impossible to analyze in the real circumstances. Compared to experimental methods, the use of this agent-based model has the convenience of saving time and economic resources. The experiments discussed in this section have as objective to show the characteristics of the model and the results that it can provide. Assuming the current unprecedented situation, extensive analysis has not been possible in order to put available the modeling tool for evaluating the risk for COVID-19.

4.1. First experiment. Basic performance

In the first experiment, the model is tested considering a population of 500 (A) susceptible agents with only one infected individual (B). In the test, it is considered a facility with the following dimensions 300× 300 ($L_x = 0$, $U_x = 300$, $L_y = 0$, $U_y = 300$). The pre-specified lower (l_{in}) and upper (u_{in}) infection probability limits are configured so that $l_{in} = 0.1$ and $u_{in} = 0.3$, which corresponds to a realistic interval considering that the average infection probability is 0.2 [32–34]. The pre-specified lower (l_{cm}) and upper (u_{cm}) contact and mobility probability limits are set so that $l_{cm} = 0.2$ and $u_{cm} = 0.4$, which represent the most frequent levels of mobility in companies or universities [35,36]. The probability of local or long-distance movement α is considered as 0.8, while the permissible perturbation is set to $S = 2mts$. The value of $R = 1$ emulates the average permissible contact level under contagious risk considered by the World Health Organization [37]. The complete simulation is executed during 500 iterations (*maxiter*).

Fig. 5 shows the agent interaction results in different iterations of the simulation process. For the sake of visualization, the size of each agent in the Figures has been exaggerated. From the Figure, it is clear how the infection is transmitted agent by agent as the number of iterations increments. In the beginning, the number of infected is low. However, the contagious is accelerated from the 100 iterations. Fig. 6 exhibits the number of infected agents$|\mathbf{B}(k)|$ in each iteration, while Fig. 7 shows the rate of infected. Fig. 6 also shows that all agents from **A** get infected from the 350 iterations. A close inspection of Fig. 7 indicates that the peak of contagious is around 150 iterations with approximately 11 infected.

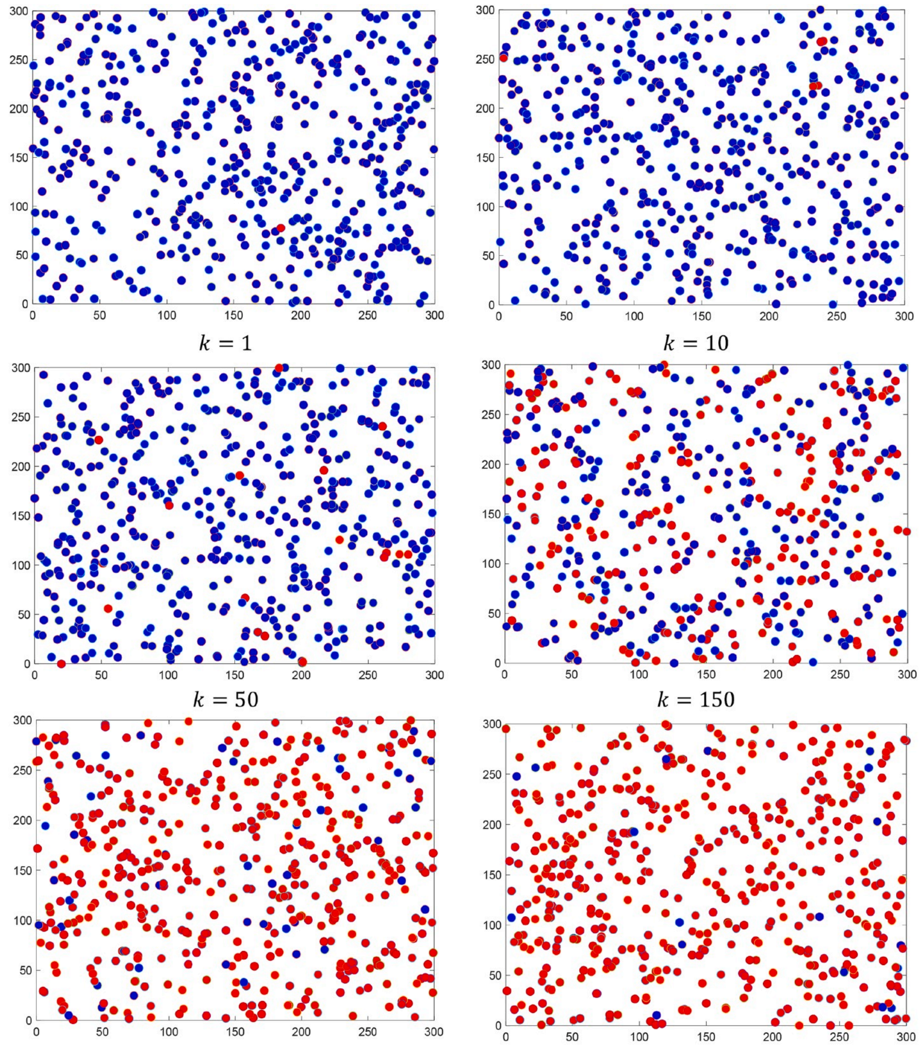

$k = 1$ $k = 10$

$k = 50$ $k = 150$

$k = 200$ $k = 300$

Fig. 5. Results in different iterations of the simulation process. Blue circles correspond to susceptible individuals, whereas red circles represent infected agents. (For interpretation of the references to colour in this figure legend, the reader is referred to the Web version of this article.)

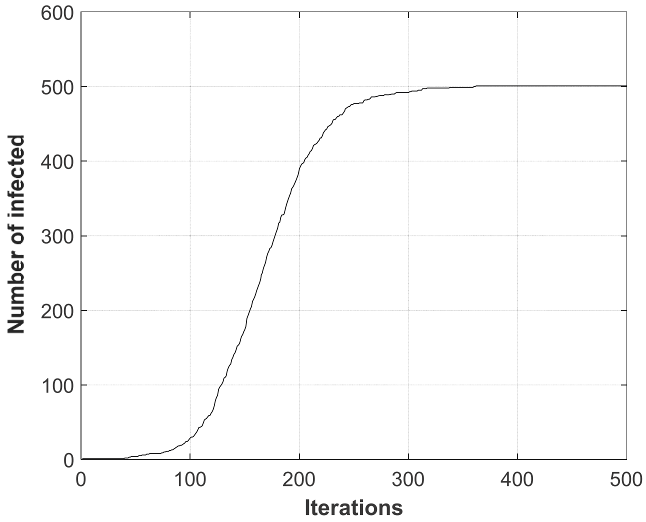

Fig. 6. Evolution of the simulation in terms of the number of infected agents.

4.2. *Outbreak endpoint*

In the next experiments, it has tested the model under different scenarios that involve the number of susceptible agents A (determining the maximal capacity of individuals in a facility maintaining a low risk) low probabilities of infection (evaluating the risk when individuals follow correct prevention practices) and the change of probabilities of contact and mobility (the influence of restricting the mobility among the individuals inside the facility). In order to evaluate the results, the iteration in which all susceptible agents A have been infected cannot be used as an informative index under the perspective that several agents could have a very low probability of infection. Therefore, the number of iterations necessary to infect most of the agents could be higher than necessary to assess the outbreak endpoint.

The problem of determining the outbreak endpoint P, which characterizes the representative outbreak size, is similar to detect the knee point in system engineering. The knee location represents the “right decision point” [38] at which the relative value of a variable is no longer significant in terms of its final contribution. There exist a few approaches for detecting knee points reported in the literature [38,39]. From them, in this paper, we use the method introduced in Refs. [38] due to its simplicity. Under this scheme, the information of the number of infected agents$|\mathbf{B}(k)|$ and iterations k produced by the simulation are

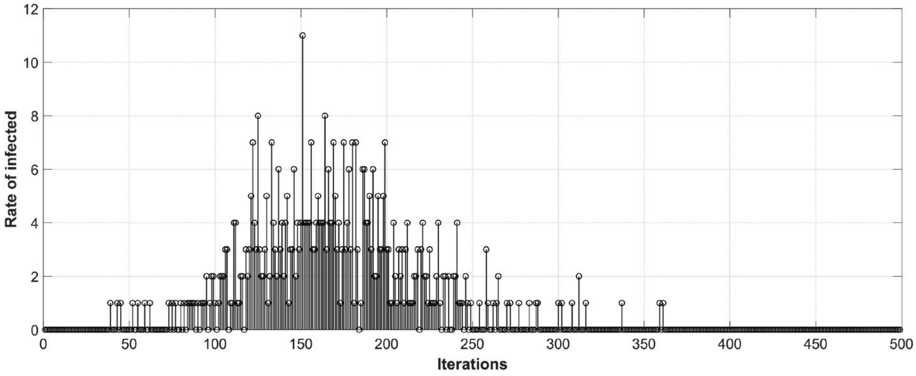

Fig. 7. Rate of infected.

normalized so that their values range from 0 to 1. This normalization process generates new sequences denoted by $|\mathbf{B}_N(k)|$ and k_N transformed as follows:

$$|\mathbf{B}_N(k)| = \frac{|\mathbf{B}(k)|}{A+B}$$
$$k_N = \frac{k}{maxiter} \tag{4}$$

Considering these normalized data, a new cost function J is formulated, which relates the number of infected agents $|\mathbf{B}_N(k)|$with regard to its significance in the evolution process (iteration k_N). This function is computed such as

$$J = |\mathbf{B}_N(k)| - k_N \tag{5}$$

One important characteristic of the function J is that it possesses only one global maximum M. This value β corresponds to the knee point. The cost function J is a sequence of size *maxiter*. Therefore, the maximal value can be obtained as follows:

$$M = \arg \max_{1 \le h \le maxiter} J(h) \tag{6}$$

Fig. 8 illustrates an example of the determination of the knee point. Fig. 8(a) shows the number of infected agents $|\mathbf{B}_N(k)|$ produced by the agent-based model. Fig. 8(b) exhibits the cost function J produced from $|\mathbf{B}_N(k)|$. As is denoted by Eq. (6), the maximal value of J corresponds to the outbreak endpoint P.

4.3. Second experiment. Size of susceptible agents

In the second experiment, the model is tested considering different population sizes of susceptible agents (A). In the test, a certain population size **A** is simulated while the outbreak endpoint P is registered. The main idea is to determine the maximal capacity of individuals that the facility can maintain without presenting a high risk considering its low transmission rates. In the test, it is considered a facility with the following dimensions 300 × 300 ($L_x = 0$, $U_x = 300$, $L_y = 0$, $U_y = 300$). For the simulations, it is considered the same configuration of experiment 1. In each simulation, a different value of A within [10,1000] is considered. Since agent-based models are stochastic schemes, each simulation is executed repeatedly 30 times. Fig. 9 shows the average results of this experiment. After analyzing Fig. 9, it can be

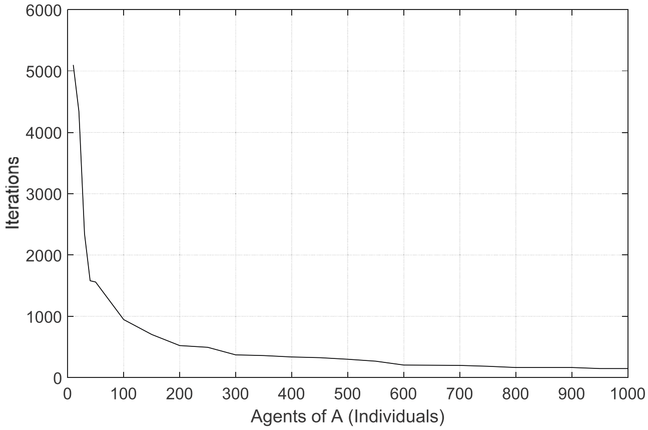

Fig. 9. Averaged results for the experiment to determine the capacity of the facility.

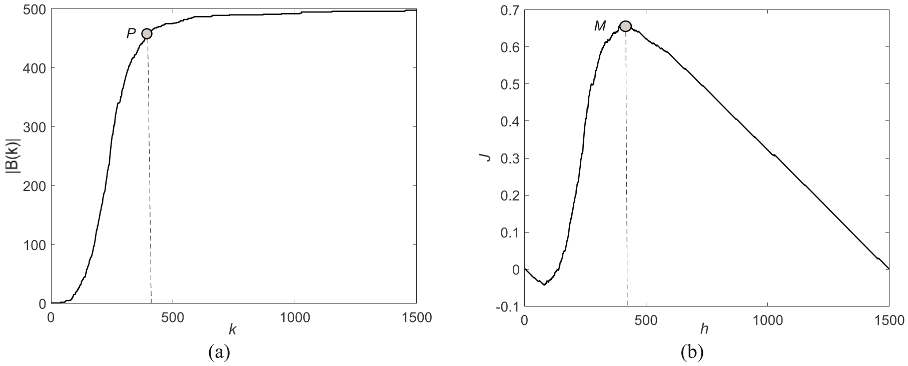

Fig. 8. Illustration of an example for the determination of the knee point (a) data produced by the simulation (b) cost function J.

seen that less than 100 individuals produce a high number of iterations, which means low transmission rates. Under such conditions, the facility is able to maintain less than 100 individuals with very low risk. On the other hand, when the number of individuals is higher than 300, the rates of transmission are practically the same.

4.4. Third experiment. Low infection probabilities

In the third experiment, the model is tested to consider the effect that the prevention measurements have for diminishing the COVID-19 transmission within the facility. The good practices considered to avoid the transmission of COVID-19 involve simple habits such as washing one's hands continuously, sneezing into one's hand or elbow and using a face mask. The observance of such simple rules reduces significatively infection probability. In the test, it is evaluated the consequences that a percentage of the agent population follows the rules and thus reduces its infection probabilities. In the experiment, at each simulation, a percentage of agents (from 0 to 100%) with low infection probability is induced in the population. Under such conditions, each agent $\mathbf{a}_i$ from $\mathbf{A}$ belongs to one of two classes: I and II. The infection probability (Pri_i) of agents from class I is generated with random numbers between the lower ($l_{in} = 0.1$) and upper ($u_{in} = 0.3$) infection probability limits. Agents from type II have been configurated considering a low probability (0.05) and deliberately induced inside the population. The rest of the model parameters maintain the same values as experiment 1. Fig. 10 shows the averaged results of this experiment (30 different independent executions). After analyzing Fig. 10, it can be seen that more than 60% of the individuals produce a high number of iterations, which means low transmission rates. Therefore, if more than 60% of the individuals in the facility are cooperative and follow the rules, the risk of transmission is drastically reduced.

4.5. Fourth experiment. Mobility restriction

In the fourth experiment, the model is used to evaluate the influence of restricting mobility among the individuals inside the facility. As has been described, the proposed model includes two different movement types: local and long-distance displacement. Both movements emulate the basic displacements performed by individuals inside the facilities. In order to decide, the movement type performed by the individuals, a probabilistic rule is conducted. The local displacement is executed with a probability of α while a long-distance is applied with a probability of $1 - \alpha$.

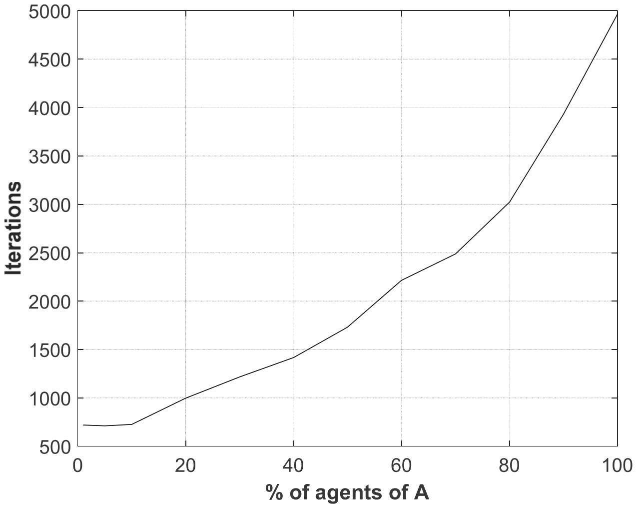

Fig. 10. Averaged results for the experiment to determine the consequences that a percentage of the agent population follows the prevention rules.

Individuals that interact within the facility can either stay in their workspace only or move to other relatively far positions through the facility (such as other departments, library, dining hall, etc.). As a hypothesis, it is considered that the restriction of mobility to allow only local interactions among individuals can reduce the risk of transmission. In order to test this hypothesis, the probabilities of our model are modified to eliminate the long-distance movements. Under such conditions, the probability α that conditions the local displacement has been set to 1. Therefore, the probability of conducting long-distance movements is zero ($1 - \alpha$).

With the objective to visualize the differences when the mobility is restricted, the experiment simulates two different cases (I) and (II). In both cases, the simulation is executed by using the same parameter values of experiment three. However, in case II, the probability α has been set to 1, eliminating the long-distance movements.

Fig. 11 shows the agent interaction results in different iterations of the simulation process for both cases. As can be seen, for the same iteration, there are many more infected agents in case I than in case II. It is also remarkable that in case II the outbreak has a local aspect. Fig. 12 illustrates the knee point for the complete simulation process for both cases in terms of the number of infected agents $\mathbf{B}(k)$. According to Fig. 12 the knee points for the case I and case II are about 500 and 5000 iterations, respectively. Under such conditions is clear that the restriction of mobility drastically reduced the transmission rate within the facility.

5. Discussion

Agent-based models are computational schemes that emulate individuals making decisions depending on a set of programmable rules. Such rules are configurated to represent the main properties of the real model. They relate the individual behavior with their social and physical profile [40]. Agent-based models are particularly important in cases in which the agent-agent interaction is an important factor in the system to be modeled. These schemes have been of prominent use to understand public health problems [41,42] and to formulate and evaluate strategies to address them. The transmission process of COVID-19 in facilities is a complex formulation whose behavior and evaluation risk depend on the interactions among the individuals rather than simply the characteristics of the individuals within the system.

Computational and Mathematical approaches have been broadly employed by researchers to model the transmission diffusion of a disease. Most of the existing schemes, such as Susceptible-Infect-Susceptible (SIS) [7], Susceptible-Infect-Recovered (SIR) [8], Susceptible-Infect-Vaccination-Susceptible (SIVS) [9] and Susceptible-Infect-Quarantine-Susceptible (SIQS) [10], consider the transmission mechanism alone, assuming a 'passive' population of individuals that do not participate in the transmission process with their personal social and health profiles. Different from such schemes, in our approach, simulated agents make decisions depending on the programmed rules. Such rules correspond to spatial patterns and infection conditions under which agents interact to characterize the transmission process. Our model also includes a personal profile for each agent (modeled in the parameters l_{in}, u_{in}, l_{cm}, u_{cm} and α), which defines its main social (spatial) and physical (health) characteristics. Agents act during the transmission process by modifying their decisions as the conditions around them change. Heterogeneity is also an essential part of our model since different agents in the same circumstances can make different decisions and the same agent in different situations can make different decisions. Even our proposed model with simple interactions (rules) and individual profiles can produce behaviors that cannot be captured and analyzed from the perspective of approaches that consider independent or passive individuals such as the SIS, SIR, SIVS and SIQS models.

Statistical methods and schemes based on regression [3,4] describe the transmission process of a disease through the relationship between

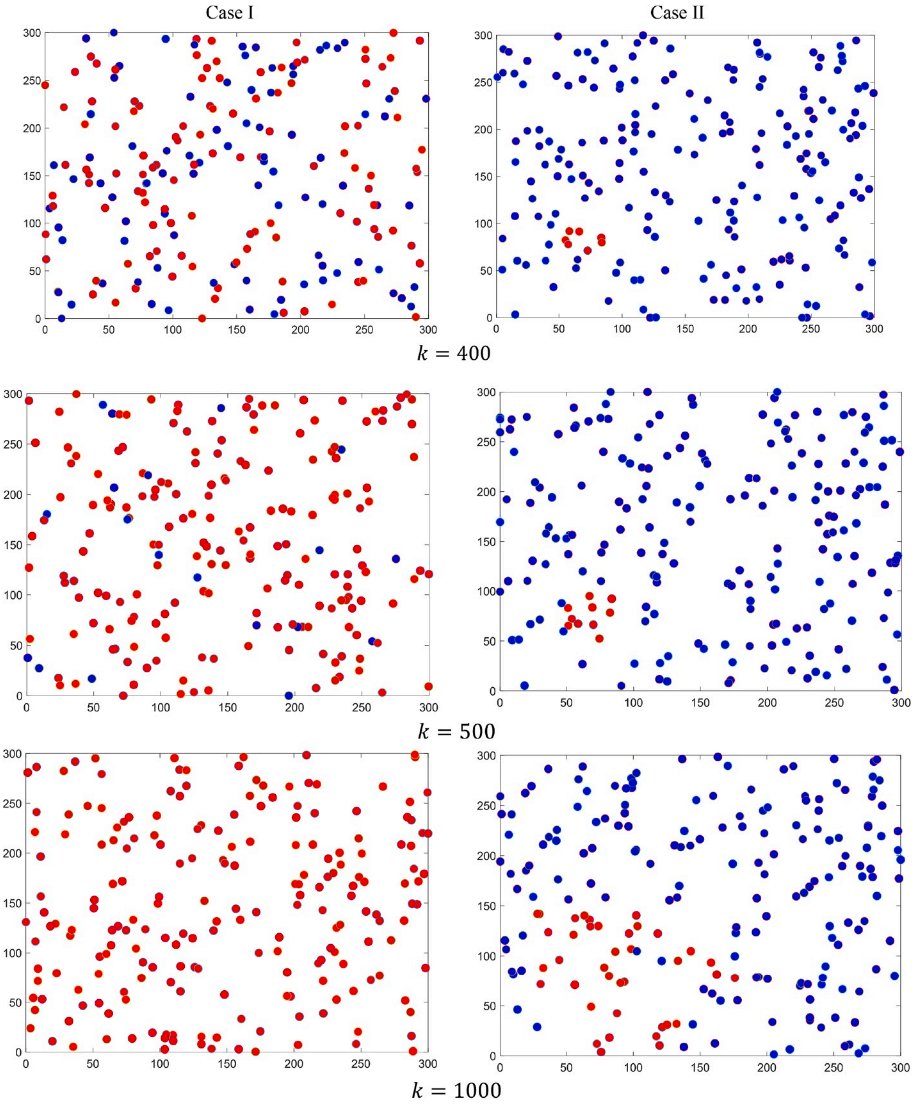

Fig. 11. Results in different iterations of the simulation process for the case I and case II. Blue circles correspond to susceptible individuals, whereas red circles represent infected agents. (For interpretation of the references to colour in this figure legend, the reader is referred to the Web version of this article.)

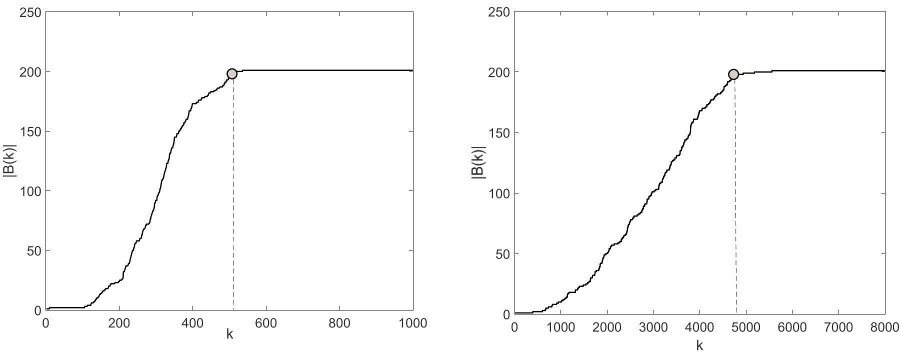

(a) Case I

(b) Case II

Fig. 12. Knee points for the complete simulation process for cases I and II in terms of the number of infected agents $\mathbf{B}(k)$.

aggregate variables that link the proportion of people in a determined condition such as susceptible or infected considering fast counts without specifying the causal connections between the variables. In contrast, in our approach, the model directly captures causal effects through the agent interactions over time. Models such as the SIS, SIR, SIVS and SIQS [7–10] based on differential equations are capable of characterizing causal relationships. However, they also adopt aggregate variables while the causal effects are described on a large scale from a macro perspective. In contrast to these schemes, our approach allows effectively to model the transmission process and causal relations with the use of micro-level interactions (agent-to-agent) considering the heterogeneity of its agent characteristics.

Agent-based models have also been used as an alternative to classical mathematical tools to describe the behavior of diseases [20–26]. These models typically consider a synthetic population divided into different sections. Each section represents a particular agent condition such as susceptible agents, infected individuals and recovered agents. Since these schemes describe the behavior of the disease in a complete country, the contact among the agents is modeled sectionally. Therefore, the models implemented in these approaches [20–26] emulate the behavior of agents with a very low heterogeneity since the characteristics of the agents are not defined individually but in a group. Under such conditions, details in the emulation of the transmission process are not modeled reliably by these approaches. Different from these models, our scheme defines each agent individually with its own personal profiles of infection and mobility. Therefore, our approach is able to produce detailed spatiotemporal simulations agent by agent. As a consequence, our scheme allows potentially a high representation of the transmission process being modeled. Thus, conclusions of the model behavior can be extrapolated to real-world, which allows insights from the model to be used to understand the system and compare different hypothetical scenarios. From the simulation of these scenarios, it can be obtained coexistence conditions that need to be imposed among the members or the habits that have to be avoided for reducing the transmission risks.

In our study, several hypothetical scenarios have been considered to show the performance of our proposed model. In Section 4.3, the model has been tested considering different population sizes of susceptible agents (A). In the test, a certain population size $\mathbf{A}$ was simulated while the outbreak endpoint P is registered. The main idea has been to determine the maximal capacity of individuals that the facility can maintain without presenting a high risk considering its low transmission rates. In Section 4.4, in the experiment, at each simulation, a percentage of agents (from 0 to 100%) with low infection probability is induced in the population. This condition can represent a determined number of individuals who do not follow good practices to avoid the transmission of COVID-19 (the use of a face mask). From the simulations, it can be evaluated the risk if a determined number of agents do not use the mask due to their work restrictions (the need the face free such as welders) or because they simply forget it. Therefore, it can be established penalties or strategies that avoid this bad observance. In Section 4.5, In the experiment, the model is used to evaluate the influence of restricting mobility among the individuals inside the facility. From this scenario, it can be evaluated the transmission effects produced for two different conditions. First, individuals stay in their workspace only (with local movements around this position). Second, the agents can move to other relatively far positions through the facility (such as other departments, library, dining hall, etc.). From the simulation results, it can be evaluated the risk of each mobility type in order to generate strategies that promote those mobilities that produce lower risks (eliminate the contact between certain departments, to choose only one person to deliver the product from one station to another, etc.).

In the design of an agent-based model, the challenge is typically expressed as a question of balance, finding relatively simple rules that capture the main characteristics of the system while also produce a detailed description of the system to be modeled. Complex rules (too much detail) are counter-productive since they obscure the connection between the agent interaction and the model behavior. One of the main characteristics of our model is simplicity. As a consequence of this simplicity, the model maintains some limitations. Since our proposed scheme is a model to evaluate the risk of infection, it does not implement the behavior of the complete disease, such as the inclusion of recovered individuals. Under such conditions, it is not possible to asses the way in which the risk decreases when recovered individuals are not able to transmit the disease. The rules implemented in our model are very simple in order to highlight the relationship between agent interaction and model behavior. As a result, several complex interactions among agents are not modeled. One case can be the influence of some individuals (skeptics) to others to act contrary to the good habits for avoiding disease transmission. Another can be the dynamic modification of the infection probability. This fact models the different risks produced for distinct health conditions (more susceptibility provoked by bad feeding or sleep disorders).

6. Conclusions

COVID-19 has become a global threat affecting almost all countries in the world. The public health consequences of acquiring COVID-19 have led many governments to impose a set of control measures. Inside facilities, there is a higher probability of infection. Within these spaces, there is maintained a high contact rate between people sharing the same common surfaces of interaction. However, rarely are there specific countermeasures related to these facilities or conducted studies that analyze possible coexistent strategies.

In this paper, an agent-based model to evaluate the COVID-19 transmission risks in facilities has been presented. In the model, the behavior of each individual is characterized by a set of simple rules that considers its basic interactions inside the facility. In its iterations, each agent maintains different mobility requirements and contagion susceptibility. From these models, several possible scenarios can be tested to obtain the coexistence conditions that need to be imposed among the members or the habits that have to be avoided for reducing the transmission risks.

The model is flexible and allows testing several hypotheses. Under this role, it is possible to test different scenarios considering distinct hypothetical conditions that are impossible to analyze under real circumstances. Compared to experimental methods, the use of this agent-based model has the convenience of saving time and economic resources. In the paper, several experiments with the model are described and discussed. The experiments have as objectives to show the characteristics of the model and the results that it can provide.

Ethical procedure

The research meets all applicable standards with regard to the ethics of experimentation and research integrity, and the following is being certified/declared true.

As an expert scientist and along with co-authors of concerned field, the paper has been submitted with full responsibility, following due ethical procedure, and there is no duplicate publication, fraud, plagiarism, or concerns about animal or human experimentation.

Declaration of competing interest

None of the authors of this paper has a financial or personal relationship with other people or organizations that could inappropriately influence or bias the content of the paper.

It is to specifically state that “No Competing interests are at stake and there is No Conflict of Interest” with other people or organizations that could inappropriately influence or bias the content of the paper.

References

[1] Gang Li, Rui Hu, Xuefang Gu, A close-up on COVID-19 and cardiovascular diseases, Nutr. Metabol. Cardiovasc. Dis. (2020), https://doi.org/10.1016/j.numecd.2020.04.001.

[2] Noelle Breslin, Caitlin Baptiste, Cynthia Gyamfi-Bannerman, Russell Miller, Dena Goffman, COVID-19 infection among asymptomatic and symptomatic pregnant women: two weeks of confirmed presentations to an affiliated pair of New York City hospitals, Am. J. Obstet. Gynecol. MFM (2020), https://doi.org/10.1016/j.ajogmf.2020.100118. In press.

[3] Michael Y. Li, An Introduction to Mathematical Modeling of Infectious Diseases, Springer Verlag, 2018.

[4] Marcello Marinia, Cyril Brunner, Ndaona Chokani, RezaS. Abhari, Enhancing response preparedness to influenza epidemics: agentbased study of 2050 influenza season in Switzerland, Simulat. Model. Pract. Theor. 103 (2020) 102091.

[5] M. Oliver, Nathan Harding Cliff, E. Mahendra Piraveenan, Yagmur Erten, Manoj Gambhir, Mikhail Prokopenko, Investigating spatiotemporal dynamics and synchrony of influenza epidemics in Australia: an agent-based modelling approach, Simulat. Model. Pract. Theor. 87 (2018) 412–431.

[6] Yan Li, Qimin Zhang, The balanced implicit method of preserving positivity for the stochastic SIQS epidemic model, Physica A 538 (2020) 122972.

[7] W. Kermack, A. McKendrick, Contributions to the mathematical theory of epidemics (Part I), Proc. R. Soc. 115 (1927) 700–721.

[8] N. Bailey, The mathematical theory of infectious diseases and its applications, Griffin 28 (1975) 479–480.

[9] J. Arino, C.C. McCluskey, P. wan den Driessche, Global results for an epidemic model with vaccination that exhibits backward bifurcation, SIAM J. Appl. Math. 64 (2003) 260–276.

[10] X. Zhang, H. Xiang, X. Meng, Dynamics of the deterministic and stochastic SIQS epidemic model wiht non-linear incidence, Appl. Math. Comput. 243 (2014) 546–558.

[11] H. Qi, S. Zhang, X. Meng, H. Dong, Periodic solution and ergodic stationary distribution of two stochastic SIQS epidemic systems, Physica A 508 (223–241) (2018).

[12] Uri Wilensky, William Rand, An Introduction to Agent-Based Modeling Modeling Natural, Social, and Engineered Complex Systems with NetLogo, MIT Press, 2010.

[13] Sven Banisch, Markov Chain Aggregation for Agent-Based Models, Springer Verlag, 2016.

[14] C. Macal1, M. North, Tutorial on agent-based modelling and simulation, J. Simulat. 4 (2010) 151–162.

[15] Macal, CM. Emergent structures from trust relationships in supply chains. In: Macal C, Sallach D and North M (eds). Proceedings of Agent 2004: Conference on Social Dynamics: Interaction, Reflexivity and Emergence. Argonne National Laboratory: Chicago, IL, 7–9 October, pp 743–760.

[16] W.B. Arthur, S.N. Durlauf, D.A. Lane (Eds.), The Economy as an Evolving Complex System II, SFI Studies in the Sciences of Complexity, Addison-Wesley, Reading, MA, 1997.

[17] V.A. Folcik, G.C. An, C.G. Orosz, The basic immune simulator: an agent-based model to study the interactions between innate and adaptive immunity, Theor. Biol. Med. Model. 4 (39) (2007). http://www.tbiomed.com/content/4/1/39.

[18] T.A. Kohler, G.J. Gumerman, R.G. Reynolds, Simulating ancient societies, Sci. Am. 293 (1) (2005) 77–84.

[19] M. North, et al., Multi-scale agent-based consumer market modeling, Complexity 15 (2009) 37–47.

[20] T.C. Germann, K. Kadau, I.M. Longini, C.A. Macken, Mitigation strategies for pandemic influenza in the United States, Proc. Natl. Acad. Sci. Unit. States Am. 103 (15) (2006) 5935–5940.

[21] I.M. Longini, A. Nizam, S. Xu, K. Ungchusak, W. Hanshaoworakul, D.A. Cummings, M.E. Halloran, Containing pandemic influenza at the source, Science (New York, N. Y.) 309 (5737) (2005) 1083–1087.

[22] T. Smieszek, M. Balmer, J. Hattendorf, K.W. Axhausen, J. Zinsstag, R.W. Scholz, Reconstruction the 2003/2004 H3N2 Influenza Epidemic in, 2003.

[23] M. Eichner, M. Schwehm, N. Wilson, M.G. Baker, Small Islands and Pandemic Influenza: Potential Benefits and Limitations of Travel Volume Reduction as a Border Control Measure, 2009, https://doi.org/10.1186/1471-2334-9-160.

[24] D. Balcan, V. Colizza, B. Gonçalves, H. Hu, J.J. Ramasco, A. Vespignani, Multiscale mobility networks and the spatial spreading of infectious diseases, Proc. Natl. Acad. Sci. Unit. States Am. 106 (51) (2009) 21484–21489. December. Available at: http://www.pnas.org/content/pnas/early/2009/12/11/0906910106.full.pdf. (Accessed 29 July 2018).

[25] O.M. Cliff, N. Harding, M. Piraveenan, E.Y. Erten, M. Gambhir, M. Prokopenko, Investigating Spatiotemporal Dynamics and Synchrony of Influenza Epidemics in Australia: an Agent-Based Modelling Approach Simulation Modelling Practice and Theory, vol. 87, 2018, pp. 412–431, 7.

[26] Marcello Marini, Cyril Brunner, Ndaona Chokani, S. Reza, Abhari, Enhancing response preparedness to influenza epidemics: agentbased study of 2050 influenza season in Switzerland, Simulat. Model. Pract. Theor. 103 (2020) 102091.

[27] Chan, V., Son, Y., Macal, C., Agent-based simulation tutorial - simulation of emergent behavior and differences between agent-based simulation and discrete-event simulation, Proceedings of the 2010 Winter Simulation Conference B. Johansson, S. Jain, J. Montoya-Torres, J. Hugan, and E. Yücesan, eds.

[28] T.C. Schelling, Dynamic models of segregation, J. Math. Sociol. 1 (2) (1971) 143–186.

[29] Hiroki Sayama, Introduction to the Modeling and Analysis of Complex Systems, Open SUNY Textbooks, Milne Library, 2015.

[30] Summer Chavez, Brit Long, Alex Koyfman, Stephen Y. Liang, Coronavirus Disease (COVID-19): a primer for emergency physicians, Am. J. Emerg. Med. In press, corrected proof Available online 24 March 2020., https://doi.org/10.1016/j.ajogmf.2020.100118.

[31] Saima Hamid, Mohammad Yaseen Mir, Gulab Khan Rohela, Novel coronavirus disease (COVID-19): a pandemic (epidemiology, pathogenesis and potential therapeutics), New Microbes and New Infections 35 (May 2020). Article 100679.

[32] Y. Huang, L. Yang, H. Dai, F. Tian, K. Chen, Epidemic Situation and Forecasting of COVID-19 in and outside China [Preprint], Bull World Health Organ, 16 March 2020, https://doi.org/10.2471/BLT.20.255158. E-pub.

[33] Lei Luo, Dan Liu, Xin-long Liao, Xian-bo Wu, Qin-long Jing, Jia-zhen Zheng, Fang-hua Liu, Shi-gui Yang, Bi Bi, Zhi-hao Li, Jian-ping Liu, Wei-qi Song, Wei Zhu, Zheng-he Wang, Xi-ru Zhang, Pei-liang Chen, Hua-min Liu, Xin Cheng, Miao-chun Cai, Qing-mei Huang, Pei Yang, Xin-fen Yang, Zhi-gang Huang, Jin-ling Tang, Yu Ma, Chen Mao, Modes of contact and risk of transmission in COVID-19 among close contacts, Am. J. Obstet. Gynecol. MFM (2020), https://doi.org/10.1101/2020.03.24.20042606. In Press.

[34] World Health Organization, Modes of transmission of virus causing COVID-19: implications for IPC precaution recommendations, Retrieved from, https://www.who.int/news-room/commentaries/detail/modes-of-transmission-of-virus-causing-covid-19-implications-for-ipc-precaution-recommendations.

[35] MahendraWardhana, Spatial analysis of users movement pattern and its socialization on public facilities and environment through the ESVA, Procedia - Social and Behavioral Sciences 227 (2016) 101–106.

[36] Jesper Steen, Henrik Markhede, Spatial and social configurations in offices, Journal of Space Sintax 1 (1) (2010) 121–132.

[37] World Health Organization, Coronavirus disease (COVID-19) outbreak, Retrieved from, https://www.who.int/home.

[38] V. Satopa, J. Albrecht, D. Irwin, B. Raghavan, Finding a "kneedle" in a haystack: detecting knee points in system behavior, in: 31st International Conference on Distributed Computing Systems Workshops, 2011, pp. 166–171.

[39] Q. Zhao, M. Xu, P. Fränti, Knee point detection on bayesian information criterion, in: 20th IEEE International Conference on Tools with Artificial Intelligence, 2008, pp. 431–438.

[40] Jennifer Badham, Edmund Chattoe-Brown, Nigel Gilbert, Zaid Chalabi, Ruth F. Hunter, Kee Frank, Developing agent-based models of complex health behaviour, Health Place 54 (2018) 170–177.

[41] A.M. El-Sayed, P. Scarborough, L. Seemann, S. Galea, Social network analysis and agent-based modeling in social epidemiology, Epidemiol. Perspect. Innovat. 9 (1) (2012) 1.

[42] Z. Chalabi, T. Lorenc, Using agent-based models to inform evaluation of complex interventions: examples from the built environment, Prev. Med. 57 (5) (2013) 434–435.